Developmental Biology **211,** 238–254 (1999)
Article ID dbio.1999.9313, available online at http://www.idealibrary.com on IDEAL®

and Branching Morphogenesis during Mouse Mammary Development

Jimmie E. Fata, Kevin J. Leco,[1] Roger A. Moorehead,[1] David C. Martin, and Rama Khokha[2]

Department of Medical Biophysics and Department of Laboratory Medicine and Pathobiology, Ontario Cancer Institute, University of Toronto, Toronto, Ontario M5G 2M9, Canada

The dynamic process of mammary ductal morphogenesis depends on regulated epithelial proliferation and extracellular matrix (ECM) turnover. Epithelial cell–matrix contact closely dictates epithelial proliferation, differentiation, and survival. Despite the fact that tissue inhibitors of metalloproteinases (Timps) regulate ECM turnover, their function in mammary morphogenesis is unknown. We have delineated the spatiotemporal expression of all *Timps* (*Timp-1* to *Timp-4*) during discrete phases of murine mammary development. *Timp* mRNAs were abundant in mammary tissue, each displaying differential expression patterns with predominant localization in luminal epithelial cells. *Timp-1* mRNA was unique in that its expression was limited to the stage at which epithelial proliferation was high. To assess whether Timp-1 promotes or inhibits epithelial cell proliferation we manipulated mammary Timp-1 levels, genetically and biochemically. Down-regulation of epithelial-derived *Timp-1* in transgenic mice, by mouse mammary tumor virus promoter-directed *Timp-1* antisense RNA expression, led to augmented ductal expansion and increased number of ducts ($P < 0.004$). In these transgenics the integrity of basement membrane surrounding epithelial ducts, as visualized by laminin-specific immunostaining, was breached. In contrast to these mice, ductal expansion was markedly attenuated in the proximity of implanted recombinant Timp-1-releasing pellets (rTIMP-1), without an increase in basement membrane deposition around migrating terminal end buds. Epithelial proliferation and apoptosis were measured to determine the basis of altered ductal expansion. Luminal epithelial proliferation was increased by 55% ($P < 0.02$) in *Timp-1*-reduced transgenic mammary tissue and, conversely, decreased by 38% ($P < 0.02$) in terminal end buds by implanted rTIMP-1. Epithelial apoptosis was minimal and remained unaffected by Timp-1 manipulations. We conclude that Timps have an integral function in mammary morphogenesis and that Timp-1 regulates mammary epithelial proliferation *in vivo*, at least in part by maintaining basement membrane integrity.

Key Words: **Timps; mammary morphogenesis; transgenic mice; epithelial proliferation.**

INTRODUCTION

Mammary morphogenesis is a dynamic, yet highly ordered process involving extensive epithelial cell proliferation. This development event initiates with the onset of puberty around 4 weeks of age in mice, as systemic circulation of ovarian hormones begins (Daniel and Silberstein, 1987; Haslam, 1987; Imagawa *et al.*, 1990). Under the influence of estrogen and progesterone, epithelial penetration into adipose stroma generates a dichotomous tree pattern, which expands by linear lengthening of primary ducts, bifurcation of terminal end buds (TEBs), and secondary lateral branching. TEBs are bulbous structures located at the migrating ductal forefront and contain stem cells that proliferate and differentiate in response to hormones (Dulbecco *et al.*, 1986; Sonnenberg *et al.*, 1986). Ductal expansion is most rapid between 5 and 8 weeks of age, and by 10 weeks, there is complete infiltration of the fat by a fully developed ductal system. During growth of the ductal tree, extracellular matrix (ECM) molecules are synthesized and

[1] Contributed equally to manuscript.

[2] To whom correspondence should be addressed at the Department of Medical Biophysics, Ontario Cancer Institute, 610 University Avenue, Toronto, Ontario M5G 2M9, Canada. Fax: (416) 946-2984. E-mail: rkhokha@oci.utoronto.ca.

0012-1606/99 $30.00

deposited as basement membrane or interstitial matrix. The ECM creates physical barriers that must be penetrated to allow for TEB migration and higher orders of lateral branching (Williams and Daniel, 1983) and therefore ECM turnover is inherent to mammary morphogenesis. It is well known that ECM integrity is largely maintained by a balance between the opposing activities of extracellular matrix proteases and their inhibitors (Mignatti and Rifkin, 1993; Woessner, 1991; Gomez *et al.*, 1997). *In vitro*, the plasminogen activator/plasmin system affects mammary epithelial branching (Delannoy-Courdent *et al.*, 1998; Fauquette *et al.*, 1997; Delannoy-Courdent *et al.*, 1996) and is known to activate matrix metalloproteinases (MMPs; He *et al.*, 1986). In turn, MMPs, which can also undergo autoactivation, have been implicated as facilitators of ductal branching *in vivo* (Sympson *et al.*, 1994; Witty *et al.*, 1995); however, the functions of their inhibitors, tissue inhibitors of metalloproteinases (Timps), during this event remain unknown. By virtue of regulating MMP activity, Timps may control the rapid physical expansion of mammary ducts through extracellular matrices by limiting or focusing matrix degradation.

The four murine Timps characterized thus far are designated Timp-1, -2, -3, and -4 (Edwards *et al.*, 1986; Stetler-Stevenson *et al.*, 1989; Leco *et al.*, 1994, 1997). Timps are multifunctional proteins capable of influencing the cellular microenvironment both physically and physiologically. Beyond their direct influence on the turnover of structural matrix molecules, Timps can also affect soluble, extracellular factors. This is through the inhibition of at least three other MMP-mediated processes: the processing of cytokines (Gearing *et al.*, 1995), the degradation of growth factor binding proteins (Thrailkill *et al.*, 1995; Fowlkes *et al.*, 1994a, b), and the release of ECM-bound growth factors (Whitelock *et al.*, 1996). Inhibition of the bioavailability of growth-promoting factors suggests that Timps can limit cellular proliferation and this may be the basis of Timps' ability to suppress primary tumor growth (Khokha, 1994; Kruger *et al.*, 1997; Montgomery *et al.*, 1994). In contrast to these effects, Timps-1 and -2 have been shown to exert mitogenic effects *in vitro* (Stetler-Stevenson *et al.*, 1992; Bertaux *et al.*, 1991; Hayakawa *et al.*, 1992, 1994). Thus, the question remains as to whether mammary Timp expression will negatively or positively affect cellular proliferation *in vivo*.

To address this question we comprehensively mapped the temporal expression patterns and cell-specific localization of all four *Timps* during murine mammary morphogenesis. To elucidate further the role of Timps, a gain of Timp-1 function and a loss of Timp-1 function were generated in mammary tissue undergoing ductal development. We achieved this by implanting slow-release pellets containing recombinant human Timp-1 (rTIMP-1; gain of function) and by generating transgenic mice with mammary-epithelial directed *Timp-1* antisense RNA expression (loss of function). Enhanced ductal development and basement membrane dissolution was evident following an epithelial-specific loss of Timp-1 function. In contrast, a gain of function impaired local mammary ductal elongation and branching but did not alter basement membranes. Immunohistochemistry linked these developmental changes to altered proliferation, but not apoptosis. This is the first evidence to show that an *in vivo* manipulation of a single Timp, Timp-1, can regulate epithelial proliferation. We conclude that Timps play an integral role in creating an environment conducive to controlled mammary epithelial ductal progression at least in part by maintaining basement membrane integrity.

MATERIALS AND METHODS

Carmine–Alum Stained Whole Mounts

The fourth inguinal fat pads of virgin mice were removed and placed on a microscope slide for several minutes to adhere to the glass. The tissue was then defatted in Clarke's fluid (75% EtOH, 25% acetic anhydride) for 16 h. After 30 min in 70% EtOH, the tissue was stained in a carmine–alum mix (0.2% carmine, 0.5% aluminum potassium sulfate) for 16 h, followed by 4–6 h of destaining (2% HCl, 70% EtOH). After dehydration in ascending concentrations of ethanol, the tissue was cleared in toluene and whole-mount images were digitized using Northern Eclipse Software (Empix Imaging, Inc., Toronto, ON, Canada).

RNA Analysis

Total RNA was extracted from a fourth inguinal mammary fat pad as described previously (Chomczynski and Sacchi, 1987). RNA concentration was determined by measuring the OD_{260} on a DU-65 spectrophotometer (Beckman Instruments, Inc., Fullerton, CA). Equal amounts of total RNA were pooled from five mice to determine the average *Timp* mRNA levels at each time point. RNA was resolved on a 1.1% agarose/5.5% formaldehyde gel, transferred to GeneScreen Plus (NEN Research Products, Inc., Boston, MA), and sequentially hybridized with murine [α-^{32}P]dCTP-labeled DNA probes specific for *Timp-1, -2, -3,* and *-4* and 18S rRNA. ^{32}P-labeled DNA probes were generated by random priming using the Prime-It Kit (Stratagene, La Jolla, CA). Membrane prehybridization, hybridizations, and washes were performed as described (Church and Gilbert, 1984). For sequential probing, the blot was stripped in 1% SDS, 2 mM EDTA for 5 min at 80°C. Densitometry was performed using Image Quant Software (Sunnyvale, CA) based on 18S RNA as the loading control.

Protein Isolation and Gelatin Zymography

Individual mammary glands were flash-frozen in liquid nitrogen and homogenized in 500 μl of extraction buffer (1% Triton X-100, 500 mM Tris–HCl, pH 7.6, 200 mM NaCl, 10 mM $CaCl_2$). The homogenate was centrifuged at 12,000*g* for 20 min at 4°C and the supernatant stored at −20°C until needed. Protein concentration was determined using Bradford assay reagents (Bio-Rad Laboratories, Hercules, CA). Twenty micrograms of mammary protein, isolated as described above, was added to 4× sample buffer (10% SDS, 4% sucrose, 0.25 M Tris, pH 6.8) and subjected to SDS–PAGE in a 10% polyacrylamide gel containing 0.1% gelatin. After electrophoresis, the gels were maintained in 2.5% Triton X-100 for 30

min, followed by incubation for 24 h at 37°C in substrate buffer (50 mM Tris, pH 7.5, 5 mM $CaCl_2$, 40 mM NaN_3). Gels were stained in Coomassie brilliant blue for 30 min at room temperature, followed by destaining (50% methanol, 10% acetic acid). Each lane represents equally pooled mammary protein from five mice, as was done for mammary mRNA levels.

In Situ Hybridization

Strand-specific probes for *Timp-1, -2, -3,* and *-4* were generated as described previously (Harvey *et al.,* 1995). Nonradioactive riboprobes were generated by incorporating digoxygenin (DIG)-labeled UTP (Boehringer Mannheim, Laval, PQ, Canada) following the manufacturer's instructions. The incorporation of [^{35}S]UTP into radioactive probes was performed as described previously (Inderdeo *et al.,* 1996). The fourth inguinal mammary fat pads from 35-day-old virgin mice were removed, fixed for 3 h at 4°C in 4% paraformaldehyde, and embedded in paraffin. Both DIG and radioactive *in situ* hybridization were performed as previously described (Harvey *et al.,* 1995; Inderdeo *et al.,* 1996).

Elvax-40 Slow-Release Pellets

Elvax-40 pellets (a gift from Dupont, Boston, MA) were washed in several changes of 90% EtOH for 1 week and then dissolved in methylene chloride (10% w/v). Ten micrograms of purified human recombinant Timp-1 protein (Clontech, San Francisco, CA) was added to 125 μl of the Elvax solution. This mixture was spread over a 1 × 1-cm area on a glass plate, flash-frozen in liquid nitrogen for 20 min, placed at −80°C for 2 days, and then air dried at room temperature for another 2 days. This concentration of Timp-1 in Elvax pellets has been previously reported to elicit mouse mammary-specific changes during involution (Talhouk *et al.,* 1992). Squares (2 × 2 × 0.5 mm) were cut and surgically implanted into the fourth inguinal fat pad (distal to the lymph node) of 30-day-old female mice. Control pellets contained no rTIMP-1. Ten days later the fad pad including the pellet was removed for whole-mount analysis. The release of protein from these pellets was confirmed by overnight incubation of the pellets in PBS followed by PAGE and silver staining, and comparisons were made to nonimpregnated pellets.

Generation and Characterization of Transgenic Lines

An antisense *Timp-1* transgene cassette was generated to direct expression specifically to mammary tissue. Full-length *Timp-1* cDNA was cloned in the 3′ to 5′ orientation downstream of the mouse mammary tumor virus promoter (MMTV-LTR) and an untranslated v-Harvey-ras 500-bp fragment. This MMTV vector was kindly provided by Dr. W. Muller (McMaster University, Canada). Transgenic mice were generated in an FVB background using standard procedures as described (Hogan *et al.,* 1986). Two distinct founder animals (5-1 and 7-1) were identified by Southern analysis of tail DNA using a murine *Timp-1* [α-^{32}P]dCTP-labeled DNA probe. Genotyping of subsequent transgenic progeny was performed by the polymerase chain reaction (PCR), from toe DNA as template and a set of primers from exon 2 (5′-GTCATAAGGGCTAAATTCATGGG-3′) and exon 3 (5′-ACTCTTCACTGCGGTTCTGGGAC-3′) of the *Timp-1* gene. Transgene-positive animals were identified by amplification of both a 196-bp transgene fragment and a 396-bp endogenous *Timp-1* fragment. In wild-type animals, only the 396-bp fragment was evident.

To confirm transgene expression in mammary tissue, total RNA was isolated from various organs from wild-type or transgenic animals and 2.5 μg was reverse transcribed at 42°C for 1 h with Superscript reverse transcriptase (RT; Gibco, Gaithersburg, MD) and oligo(dT) primers. Ten percent of this reaction was amplified by PCR using two primer sets in the same reaction. One set was specific for the transgenic cassette and included a forward primer specific for MMTV-LTR (5′-GCCATCCCGTCTCCGCTCGTCA-CTTATC-3′) and a reverse primer specific for antisense *Timp-1* (5′-ATCCCTTGGGGCCCGATGACCTGAAG-3′). This produces a 550-bp fragment containing the entire 500-bp v-Harvey-ras region in transgene-bearing animals. The other primer set was for murine *interleukin-2* (a forward primer, 5′-CTAGGCCACAGAATTGA-AAGATCT-3′, and a reverse primer, 5′-GTAGGTGGAATTCTA-GCATCATCC-3′) and yielded a 324-bp fragment. Amplification of *interleukin-2* in the same PCR served as a positive control as it confirmed the success of PCR amplification for transgenic and wild-type animals. Southern blotting of the PCR product and subsequent probing with a cDNA specific for the v-Harvey-ras region further confirmed the identity of the transgene-specific PCR product.

RNase Protection Assay

The RNase protection assay was performed using strand-specific probes, essentially as described (Melton *et al.,* 1984). The *Timp-1* antisense probe consisted of a 155-bp internal fragment of the mouse *Timp-1* cDNA, and the GAPDH antisense probe was a 70-bp fragment of the mouse GAPDH cDNA (a gift from Dr. D. Edwards, University of East Anglia, UK). Both cDNAs were cloned into the pBluescript plasmid. Riboprobes were generated using T7 RNA polymerase in the presence of [^{32}P]UTP according to established procedure (Melton *et al.,* 1984).

The decrease in molecular weight of the probe was due to the digestion of single-stranded plasmid polylinker sequences synthesized as part of the riboprobes and demonstrated that the digestion products were specific for the *Timp-1* and GAPDH mRNAs. After electrophoresis, the gel was fixed, dried, and exposed on a phosphor screen (Molecular Dynamics, Sunnyvale, CA) for 2 h and densitometric analysis was performed using Image Quant Software (Molecular Dynamics).

Proliferating Cell Nuclear Antigen (PCNA), Laminin, and Collagen Type IV Immunohistochemistry

Mammary tissue was collected, fixed, processed, and sectioned as described for *in situ* hybridization. Sections were then dewaxed in two changes of xylene, rehydrated through an ethanol series, and placed into 3% hydrogen peroxide for 10 min to block endogenous peroxidase activity. Slides were rinsed in water and microwaved for antigen retrieval in 10 mM citrate buffer, pH 6.0, for PCNA or digested for 40 min at 42°C with pepsin (0.4%, pH 5.2, Sigma, St. Louis, MO) for laminin and collagen type IV antigen retrieval. Slides were rinsed in PBS, incubated with anti-PCNA (1:1000 dilution; Novocastra Laboratories Ltd., New Castle, UK), anti-laminin (1:500 dilution; Monosan, Uden, Netherlands), or anti-collagen type IV (1:500 dilution; Chemicon, Temecula, CA) antibodies for 1 h in a humid chamber at room temperature, and washed in PBS. Bound antibody was detected using the Level 2 Ultra Streptavidin Detection System (Signet Laboratories, Inc., Dedham, MA) and fresh AEC substrate (3-amino-9-ethylcarbazole;

Sigma) as described by the manufacturer. Tissue was counterstained in Mayers hematoxylin, rinsed in PBS, and mounted with crystal mount (Biomeda Corp., Foster City, CA).

Bromodeoxyuridine Immunohistochemistry and Apoptosis Determination

Bromodeoxyuridine (BrdU; Sigma) was dissolved in PBS and administered by ip injection at 75 mg/kg of mouse weight. Two hours later, mice were sacrificed and mammary tissue was collected, fixed, processed, and sectioned as described for *in situ* hybridization. Sections were then dewaxed in two changes of xylene, rehydrated through an ethanol series, and rinsed in water. After being denatured in 2 N HCl at 37°C for 30 min, sections were neutralized in 0.1 M sodium borate (pH 7.0) for 5 min and then rinsed in water. Sections were then placed into 3% hydrogen peroxide for 10 min to block endogenous peroxidase activity. After a rinse in PBS, sections were blocked with Signet blocking reagent (Signet Laboratories) for 5 min. Antibody specific for BrdU (1:1000 dilution; Sigma) was added to the sections and incubated in a humid chamber for 1 h at room temperature. Detection of bound antibody was identical to the detection of anti-PCNA antibodies. Immunohistological staining of apoptotic cells was performed as described previously (Wijsman *et al.,* 1993).

Morphometric Analysis

All morphometric analyses were performed on the fourth inguinal mammary fat pad using double-coded slides. For PCNA and apoptosis, counting of positive- and negative-stained epithelial cells was performed in the area distal to the lymph node in transgenic mammary tissue. On the other hand, TEBs and subtending ducts were scored separately for BrdU-positive staining in rTIMP-1-pellet experiments. This approach was taken because the transgenic manipulation occurs throughout the tissue while separate measurements were necessary in the pellet-implanted tissue because of the differential proximity of TEBs and subtending ducts to rTIMP-1-releasing pellets. Histologically, multiple serial sections defined TEBs, which were multicellular club-shaped structures located at the epithelial migrating forefront. The PCNA and BrdU indices were calculated as the number of positive epithelial cells divided by the total number of epithelial cells. An average of 1000 nuclei were scored for PCNA and apoptosis per section, while the average number of TEBs scored for BrdU was 2.5 per section, each containing no fewer than 150 nuclei. The PCNA and apoptotic indices were compared statistically using a one-tailed Student *t* test, whereas a Student *t* test for paired samples was performed on BrdU comparisons. Indices were expressed as the means ± SD.

Laminin and collagen type IV morphometry was performed on double-coded slides. To quantitate basement membrane degradation in mammary tissue, immunostaining around epithelial ducts was scored either as continuous or as discontinuous. A minimum of 40 ducts was scored for each tissue section. The percentage of discontinuous ducts in transgenics was compared to that of age-matched littermates. Student's *t* test was used to assess the significance and values were expressed as the means ± SD.

To compare the number of total ducts between transgenic and wild-type mice, we counted the ducts that bisected a randomly generated cross-sectional line in whole mounts at four distinct areas distal to the lymph node. Student's *t* test was used to assess the significance and indices were expressed as the means ± SEM.

RESULTS

Characterization of Distinct Phases of Mammary Morphogenesis in Virgin Mice

Carmine–alum whole mounts of the fourth inguinal fat pad isolated at discrete ages (15, 25, 35, 55, 75, 95 days) clearly illustrated the progression of mammary ductal development in virgin CD1 female mice. A rudimentary ductal tree consisting of a sparse network of short ducts originated at the teat before puberty (15 days; Fig. 1A). Ductal elongation initiated at puberty (~25 days; Fig. 1B) and continued beyond the lymph node (35–55 days; Fig. 1C) until 75 days when the entire fat pad was completely infiltrated by a fully developed ductal tree. TEBs were located at the forefront of the migrating ducts and were clearly evident at 35 days (Fig. 1C). Higher orders of branching became more apparent by 55 days (Fig. 1D), while alveolar-like buds, which form secretory alveoli for milk production during lactation, were seen in mature 75-, 95-, and 140-day-old mice (Figs. 1E and 1F and data not shown). These analyses defined the phases of mammary morphogenesis as a function of age in CD1 mice.

Abundance of Timps and Their Differential Expression in Mouse Mammary Morphogenesis

We determined the temporal changes in *Timp* mRNA levels (Fig. 2A) in mammary tissue representing distinct phases of ductal development and quantified these by densitometry (Figs. 2B–2E). All four *Timps* were abundant in mammary tissue compared with their differential expression in most murine organs (Leco *et al.,* 1997). In prepubertal mice, *Timp-1* mRNA levels were negligible and *Timp-2* levels were very low, which was in contrast to high *Timp-3* and *-4* expression levels. Of the four *Timp* mRNAs, a striking 30-fold induction occurred for *Timp-1* between 15 and 35 days. This was followed by a sharp decline between 55 and 75 days that remained low in mature mammary tissue. *Timp-2* mRNA levels were maximal at day 55, remaining high until 95 days, and declined in 140-day-old tissue. *Timp-3* and *Timp-4* messages were abundant through all stages, but their levels were also reduced in 140-day-old mammary tissue. Analysis of *Timp* mRNA levels from individual mice, normalized against 18S rRNA, revealed temporal expression patterns identical to those presented in Fig. 2 (data not shown). As well, the induction of *Timp-1* observed at 35 days proved to be highly significant ($P < 0.005$). Intriguingly, message levels of *Timp-3* and *-4* were down-regulated at this age. The narrow window of *Timp-1* expression, limited to the stage of active epithelial proliferation, suggested a unique role for this family member during mammary morphogenesis, even though based on exposure times this *Timp* was lower in abundance compared to others. Further, the reduction of all *Timps* beyond day 95 correlated with the completion of the majority of ECM turnover in virgin mammary development by this age.

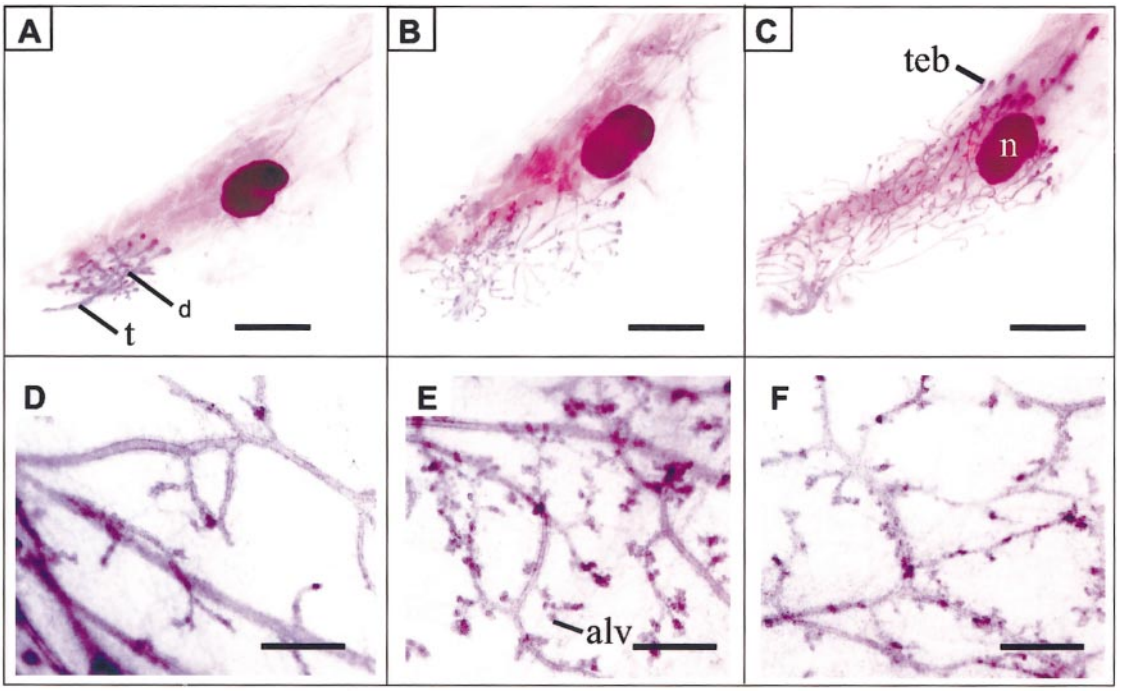

FIG. 1. Stages of mammary ductal development in virgin CD1 female mice visualized by carmine–alum whole-mounts. Early ductal expansion is evident at low magnification (A–C) and the extent of branching in older tissue is seen at higher magnification (D–F). (A) Prepubertal 15-day-old tissue with teat (t) and rudimentary ductal tree (d). (B) 25-day-old tissue at the onset of puberty. (C) Abundance of terminal end buds (teb) in the rapidly expanding ductal tree at 35 days. Most TEBs localized immediately distal to the lymph node (n). (D) Higher orders of branching are evident in 55-day-old tissue. Alveolar-like buds (alv) are present after ductal elongation ceases in 75- (E) and 95-day-old (F) tissue. Scale bars, (A–C) 2 mm and (D–F) 0.25 mm.

Predominant Epithelial Localization of Timps in Mammary Tissue

To identify the mammary cell types that produce each *Timp* we performed *in situ* hybridization in 35-day-old tissue, a stage that expressed all *Timps*. Overall, each *Timp* mRNA localized predominantly to luminal epithelial cells. Some expression of *Timp-1, -3,* and *-4* was also observed in fibroblasts surrounding the ducts (Figs. 3A, 3B, 3G, and 3J, arrowhead), while *Timp-2* was exclusive to luminal epithelial cells (Figs. 3D and 3E). *Timp-3* mRNA was frequently more prominent on one side of the duct (Figs. 3G and 3H) and also localized to histologically defined myoepithelial cells (Fig. 3H, arrowhead). *Timp-4* was unique in that it was present in many mammary cell types, including the condensed cytoplasm of adipocytes and resident mononuclear interstitial cells (Fig. 3K). The specificity of the hybridization signal was confirmed using the corresponding sense-specific riboprobes, which served as negative controls (Figs. 3C, 3F, and 3L). In addition, no signal was evident in tissue pretreated with RNase A (Fig. 3I). All *Timps* were also expressed in TEBs and their cap cells (Figs. 4A–4D, arrowheads). *Timp-1, -2,* and *-4* (Figs. 4A, 4B, and 4D) were dispersed throughout the entire TEB while *Timp-3* (Fig. 4C) appeared localized only to the outermost cellular layer of the TEB, which is composed of cap cells (Daniel *et al.*, 1987). Due to the low *Timp-1* abundance, *in situ* hybridization was performed with ^{35}S-labeled *Timp-1*-specific riboprobes which allowed for increased sensitivity (Figs. 3A–3C and 4A).

Functional Identification of Gelatinase Activity during Mouse Mammary Morphogenesis

Expression of certain MMP mRNAs during mammary morphogenesis has been reported (Witty *et al.*, 1995), although MMP activity has not been reported. We examined gelatinase activity (Fig. 5) since both MMP-2 and MMP-9 are capable of degrading collagen type IV, the main component of basement membrane which surrounds all mammary epithelial ducts. MMP-2 was the predominant active gelatinase present at all time points. As early as 15 days, three gelatinolytic bands, representing pro-MMP-9 (gelatinase-B; 105 kDa), pro-MMP-2 (gelatinase-A; 68 kDa), and activated MMP-2 (60 kDa), were present in mammary tissue. Increased amounts of MMP-2 (both pro and active forms) were detected at 35 days, when pronounced ductal expansion is known to occur. Active MMP-9 (84 kDa) was

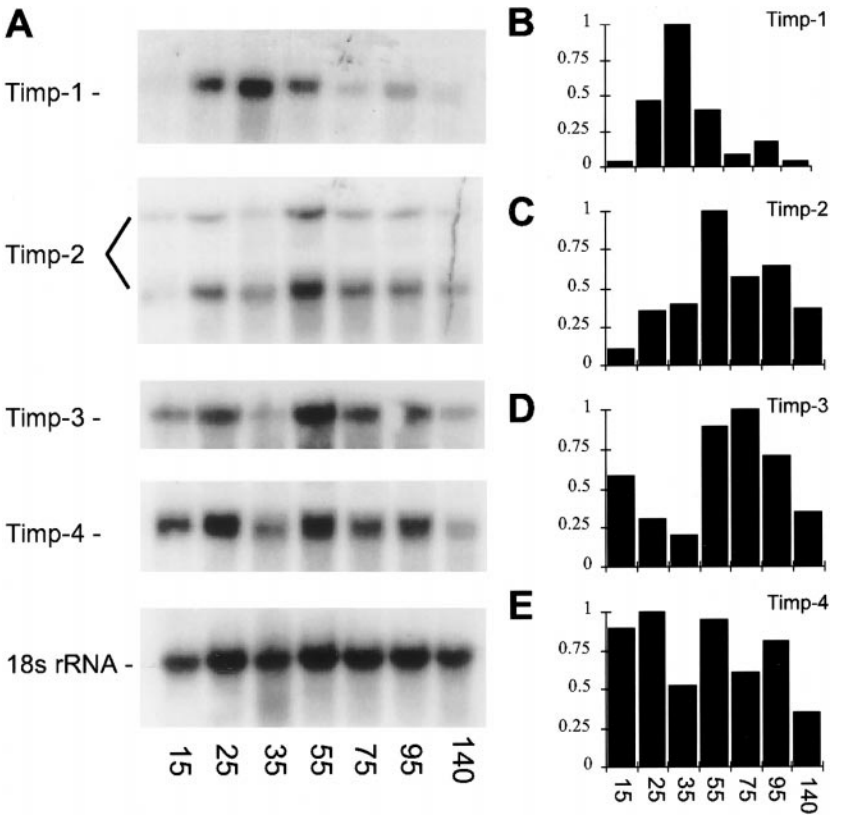

FIG. 2. Expression profiles of *Timp* mRNAs during mammary morphogenesis. (A) Northern analysis of mammary RNA isolated from virgin mice at indicated ages. 18S rRNA confirmed equivalent RNA loading. (B–E) Graphical representation of the densitometric analysis of *Timp* mRNA levels corrected for loading using 18S RNA levels.

evident from 25 days onward with maximal activity between 55 and 140 days. These results showed that gelatinases participated in virgin mammary morphogenesis and suggested that extensive basement membrane remodeling was inherent to this event. The fact that gelatinase activity existed at days 95 and 140, after ductal progression has ceased, suggested that this tissue was continually undergoing matrix turnover in the adult mouse.

Impediment of Ductal Progression by Local rTIMP-1 Elevation

Since *Timp-1* expression was restricted to a time that precisely corresponded to ductal expansion (Fig. 2B), our aim was to increase its levels and determine the direct consequence on ductal growth. This was achieved by using ethylene vinyl acetate (Elvax) polymer pellets, which are well characterized for their ability to release incorporated biomolecules over extended time periods (Langer and Folkman, 1976; Rhine *et al.*, 1980) in organs such as the mammary tissue (Jones *et al.*, 1996; Ruan *et al.*, 1995; Vassilacopoulou and Boylan, 1993; Talhouk *et al.*, 1992). Pellets impregnated with rTIMP-1 were surgically implanted immediately distal to the migrating TEBs in the fourth inguinal fat pad of 30-day-old mice. This time point was chosen as it represented active ductal expansion. We first confirmed that implanted pellets lacking rTIMP-1 (insert pellet) had no effect on ductal progression (Fig. 6A, left). Further, pellets containing rTIMP-1 implanted in one fat pad had no systemic effect on the contralateral fat pad (data not shown). We then simultaneously implanted a pellet containing rTIMP-1 in one fourth inguinal fat pad (Fig. 6B, left) and an inert pellet in the contralateral fat pad (Fig. 6B, right). The latter were ideal internal negative controls since these two mammary fat pads were exposed to identical systemic hormonal influences. We found that a local rTIMP-1 elevation had clearly impeded ductal elongation when whole-mount analysis was performed 10 days later. A strong attenuation of ductal growth was observed in the immediate vicinity of all implanted rTIMP-1 pellets (Fig. 6B, left). In comparison, inert pellets lacking rTIMP-1 had no effect in the contralateral tissue since ductal expansion proceeded normally, around and past the pellet (Fig. 6B, right). Observations for inert and rTIMP-1 pellets were reproduced in an independent experiment.

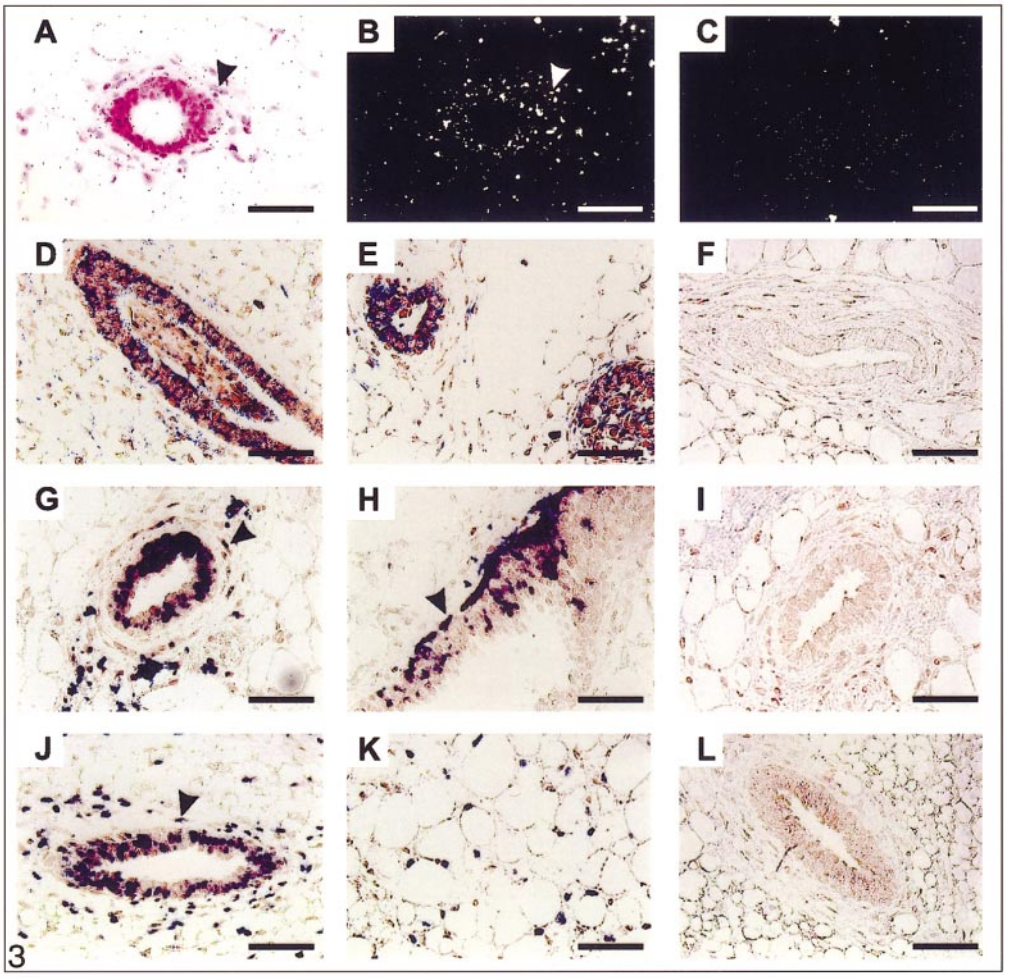

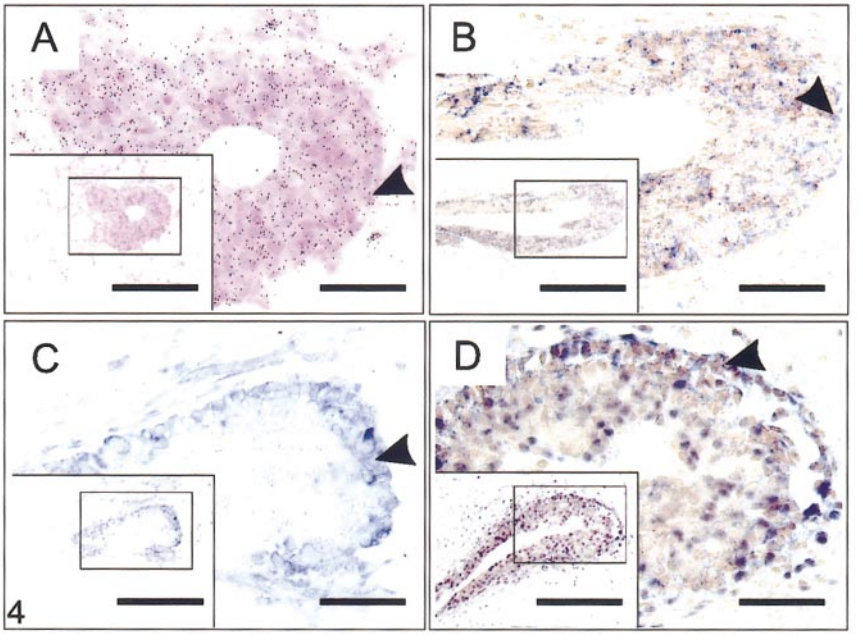

Augmented Ductal Progression in Transgenic Mice with Reduced Mammary Timp-1

We used a genetic approach to determine whether a reduction of mammary Timp-1 levels would also affect epithelial ductal growth. To reduce the epithelial cell-derived Timp-1 during mammary development in virgin mice, we expressed *Timp-1* antisense RNA from the MMTV-LTR (Fig. 7A). The MMTV promoter is constitutively active and has mammary epithelial cell specificity, with some promiscuity of expression in other glandular epithelial organs (Muller *et al.*, 1988; Pattengale *et al.*, 1989). Two independent mouse lines (5-1 and 7-1) were generated from individual transgenic founders. To detect transgene RNA expression, RT-PCR was performed in the same tube using two primer sets: transgene-specific primers and the unrelated murine *interleukin-2* gene primers. Antisense-*Timp-1* RNA was detected in transgenic mammary (Fig. 7B), spleen, and salivary gland tissues (data not shown) of both mouse lines. Samples from control littermates showed only the presence of *interleukin-2* mRNA (Fig. 7B). Strand-specific RNase protection assays confirmed the presence of antisense transcripts in transgenic mammary tissue (data not shown) and allowed us to quantify the levels of *Timp-1* mRNA in mammary tissue from transgenic and wild-type littermates (Fig. 7C). We found a significant 52% reduction of endogenous mammary *Timp-1* mRNA levels in transgenics compared to their wild-type littermates (Fig. 7C; 18.9 ± 3.4 vs 9.0 ± 3.4; $P < 0.012$). At the stage of active ductal expansion the 52% reduction of mammary *Timp-1* led to augmented ductal growth in 5-1 transgenic animals (Figs. 8A–8C, bottom) compared to their wild-type controls (Figs. 8A–8C, top). This included a more pronounced linear lengthening and migration of the ductal tree, as well as supernumerary branching. Further, the total number of epithelial ducts was significantly increased by 33% (20.4 ± 1.0 vs 15.1 ± 0.5; $P < 0.004$) compared to wild-type littermates. The number of TEBs did not differ significantly between the transgenic and the wild-type littermates. These phenotypes were also seen in the independent transgenic mouse line 7-1 that had reduced mammary *Timp-1* expression. In this line, we observed a 38% increase in the number of epithelial ducts at 50 days of age (data not shown).

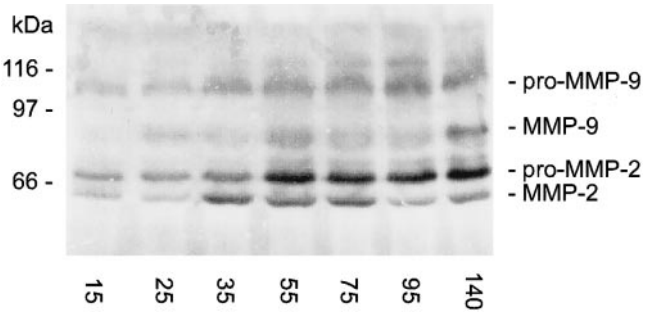

FIG. 5. Gelatin zymography in developing mouse mammary tissue. Pro-MMP-2 (progelatinase A; 68 kDa) and active MMP-2 (gelatinase A; 60 kDa) were present in 15- to 140-day-old tissue. Pro-MMP-9 (progelatinase B; 105 kDa) and active MMP-9 (gelatinase B; 84 kDa) were at lower levels compared with MMP-2, but were evident at all time points. Molecular weight markers are indicated; the negative image was generated with Adobe PhotoShop.

By 95 days of age, the transgenic and wild-type littermates did not show any overt differences at the whole-mount level. This indicated that down-regulation of *Timp-1* augmented ductal development at earlier ages, but did not cause sustained mammary hyperplasia. Mammary differences in transgenics and wild types during gestation, lactation, and involution are currently being investigated.

Discontinuous Laminin in Basement Membrane of Timp-1-Reduced Mammary Epithelial Ducts

Basement membrane integrity was assessed in mammary tissue by examining the intensity and continuity of basement membrane proteins around ductal structures (Alexander *et al.*, 1996b; Talhouk *et al.*, 1992; Martinez-Hernandez *et al.*, 1976). Immunohistochemistry on mammary tissue localized laminin and collagen type IV to the basement membranes surrounding the epithelial ducts (Figs. 9A–9H, data not shown) as well as blood and lymph

FIG. 3. Spatial localization of *Timp* mRNAs in 35-day-old virgin mouse mammary tissue using *in situ* hybridization. (A,B) *Timp-1* antisense probe detected signal within mammary ductal epithelial cells and surrounding fibroblast cells (arrowhead). (C) *Timp-1* sense probe on adjacent section with identical cellular density. (D,E) *Timp-2* antisense probe; *Timp-2* signal was exclusive to ductal epithelial cells. (F) *Timp-2* sense probe. (G,H) *Timp-3* antisense probe; *Timp-3* signal was predominant in ductal epithelial cells with some expression in the surrounding fibroblasts (arrowhead in G). It was also present in myoepithelial cells (arrowhead in H). (I) Adjacent section treated with RNase A prior to hybridization with antisense *Timp-3* probe. (J,K) *Timp-4* antisense probe; *Timp-4* signal localized predominantly to ductal epithelial cells and the surrounding fibroblasts (arrowhead in J). (K) *Timp-4* also localized to adipocytes and resident mononuclear interstitial cells. (L) *Timp-4* sense probe. (A–C) ^{35}S-labeled riboprobes; (D–L) DIG-labeled riboprobes. (A, D–L) Bright field; (B,C) dark field. (A–L) Scale bars, 50 μm.

FIG. 4. Expression of *Timp-1* to *-4* mRNA in terminal end buds during ductal development. (A) *Timp-1* and (D) *Timp-4* mRNA localized to cells scattered throughout the TEB and to surrounding stromal cells. (B) *Timp-2* mRNA localized to scattered cells throughout the TEB but not to surrounding stromal cells. (C) *Timp-3* mRNA localized to outer cell layer of TEBs and surrounding stromal cells. All *Timps* were found in cap cells (arrowheads) of TEBs. (A) ^{35}S-labeled riboprobes. (B–D) DIG-labeled riboprobes. (A–D) Scale bars, 50 μm; inset, 0.55 mm.

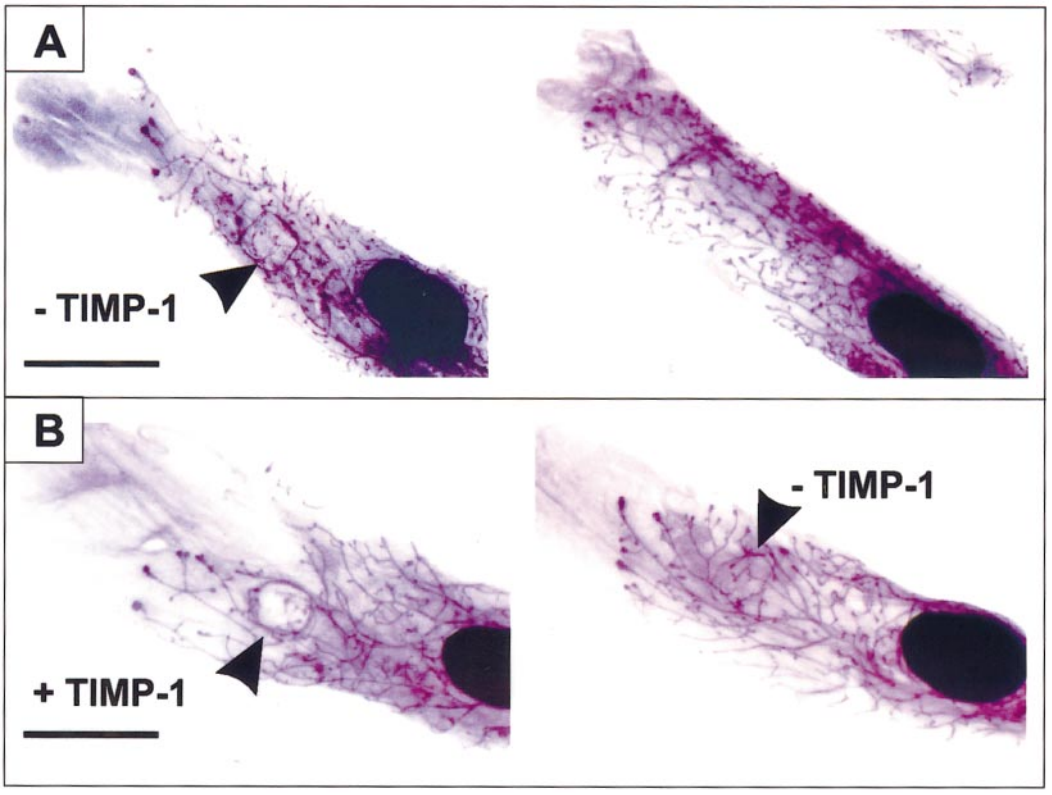

FIG. 6. Inhibition of actively growing mammary ducts with recombinant human Timp-1. (A,B) Whole-mounts of 40-day-old mice containing slow-release pellets (arrowheads) with (+TIMP-1) or without (−TIMP-1) purified rTIMP-1 that were surgically implanted at day 30. (A) Left whole mount, pellet without rTIMP-1; contralateral tissue has no pellet. (B) Left whole-mount has pellet with rTIMP-1; contralateral pellet lacks rTIMP-1. Images were captured with a stereomicroscope. Scale bars, 0.25 cm.

vessels (data not shown). We found that immunolocalization of laminin was frequently discontinuous, diffuse, or of lighter intensity in *Timp-1*-reduced tissue (Figs. 9E–9H). In these transgenics a greater than 2-fold increase ($P < 0.05$; $n = 4$) in the number of ducts that had aberrant laminin signal was observed, compared to their age-matched littermates (Fig. 9I). In three of four cases, collagen type IV was also frequently discontinuous (1.3-fold greater) and less intense in transgenics than in their wild-type controls (Fig. 9J). We next set out to determine if *Timp-1* reduction resulted in lower total stromal matrix. Utilizing Masson's trichrome staining, which histologically differentiates collagenous material, and Image Quant Software, we quantified mammary stromal matrix content. No significant difference was found in total stromal matrix content between transgenics and wild types (Fig. 9K; 12.6 ± 1.9% vs 13.8 ± 0.9%).

To determine if rTIMP-1 released from the implanted pellets affected basement membrane around TEBs we examined laminin and collagen IV immunostaining surrounding these structures. We found that both of these components of the basement membrane became gradually thinner toward the tip of the TEB, while collagen type IV was often absent at the very tip. However, no differences were apparent among TEBs migrating toward pellets releasing rTIMP-1, inert pellets, or no pellets (data not shown). Total stromal matrix content (Masson's trichrome stain) was also not affected by rTIMP-1 slow-release pellets (data not shown).

Timp-1 Affects Mammary Epithelial Proliferation but Not Apoptosis

Mammary epithelium establishes close contacts with the ECM, which then influences its survival by affecting proliferation and apoptosis (Hay, 1993). To determine the level at which Timp-1 altered ductal expansion, we measured proliferation and apoptosis in Timp-1-manipulated tissue. TEBs migrating toward rTIMP-1-releasing Elvax pellets had significantly fewer proliferating cells (an average reduction of 38%) compared to contralateral tissue in which TEBs were migrating toward an inert pellet or no pellet at all (Figs. 10A–10C; 19.2 ± 2.5% vs 27.6 ± 1.9%; $P < 0.02$). No differences were observed in luminal epithelial proliferation in subtending ducts (data not shown). The opposite scenario of increased proliferation was evident in transgenic

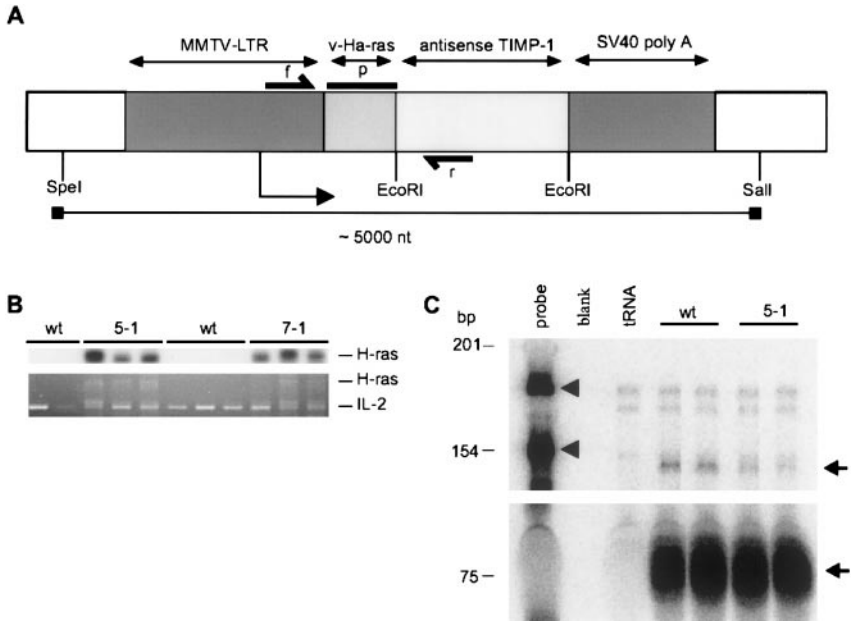

FIG. 7. Generation and characterization of MMTV-antisense *Timp-1* transgenic mice. (A) The MMTV-antisense *Timp-1* transgene construct. Unshaded regions represent the vector backbone. The MMTV-LTR and the 5′ noncoding sequences are derived from the MMTV/c-neu recombinant vector (Muller *et al.*, 1988). The *Eco*RI fragment represents the full-length encoding region of murine *Timp-1* cDNA cloned in the antisense direction. SV40 sequences provide the processing signals. Forward (f) and reverse (r) primers were used in RT-PCR to amplify transgene-specific transcripts. The v-Harvey-ras sequence (p) was used to probe Southern blots for transgene-specific sequences. (B) Reverse-transcribed total RNA from wild-type (wt) and transgenic lines (5-1 and 7-1). Samples from 55-day-old mammary tissue were concurrently amplified with f/r primers for the transgene and with a set of primers specific for *interleukin-2* (IL-2; bottom). Amplification of the latter provided internal positive control for PCR amplification. Amplified products were electrophoresed, blotted, and probed with a ^{32}P-labeled v-Ha-ras sequence (top). (C) RNase protection assay was performed using antisense riboprobes specific for *Timp-1* and GAPDH (an internal loading control). The *Timp-1* antisense riboprobe is 195 bp (top arrowhead) and its protected fragment is 150 bp (top arrow); the GAPDH riboprobe is 155 bp (bottom arrowhead) and its protected fragment is 75 bp (bottom arrow). A decreased level of *Timp-1* transcripts was evident in transgenic (5-1) versus wild-type mammary tissue.

Timp-1-reduced tissue. We found a significant increase in the number of PCNA-positive epithelial cells in 5-1 mice compared to their age-matched wild-type littermates (Figs. 10D–10F; 38.1 ± 4.6% vs 24.0 ± 1.5%; $P < 0.02$). These results demonstrated an average increase of 55% in epithelial proliferation in transgenic *Timp-1*-reduced mammary tissue.

Apoptosis assessed by *in situ* end labeling of fragmented genomic DNA was quantified in transgenic and pellet containing and their respective control tissues. Apoptosis was nonexistent in luminal epithelia during virgin mammary morphogenesis and remained unaffected by Timp-1 manipulations (data not shown).

DISCUSSION

Extensive epithelial proliferation, ductal expansion, and branching morphogenesis are processes integral to mouse mammary development. This developmental event has been known for over 70 years and is readily visualized by staining mammary fat pad whole mounts. The four distinct phases, prepuberty, onset of puberty, pronounced ductal expansion, and mature tissue with alveolar-like buds, were clearly evident during mammary development in CD1 mice (Fig. 1). In this study we have demonstrated that gelatinase activity was evident during mammary morphogenesis (Fig. 5) and that *Timps* were differentially expressed (Fig. 2), suggesting that these gene families together provide the controlled proteinase–inhibitor interactions necessary for regulated epithelial ductal growth. The *Timps* were expressed predominantly in mammary epithelial cells with some expression in stromal cells (Fig. 3). In addition, all four Timps were found in advancing TEBs (Fig. 4) and their cap cells, which are considered undifferentiated mammary epithelial cells (Daniel *et al.*, 1987) and the target cells for chemical carcinogenesis (Imagawa *et al.*, 1990). Intriguingly, *Timp-1* exhibited a narrow window of expression at the time of most rapid epithelial proliferation when *Timps-3* and *-4* were down-regulated. We used biochemical

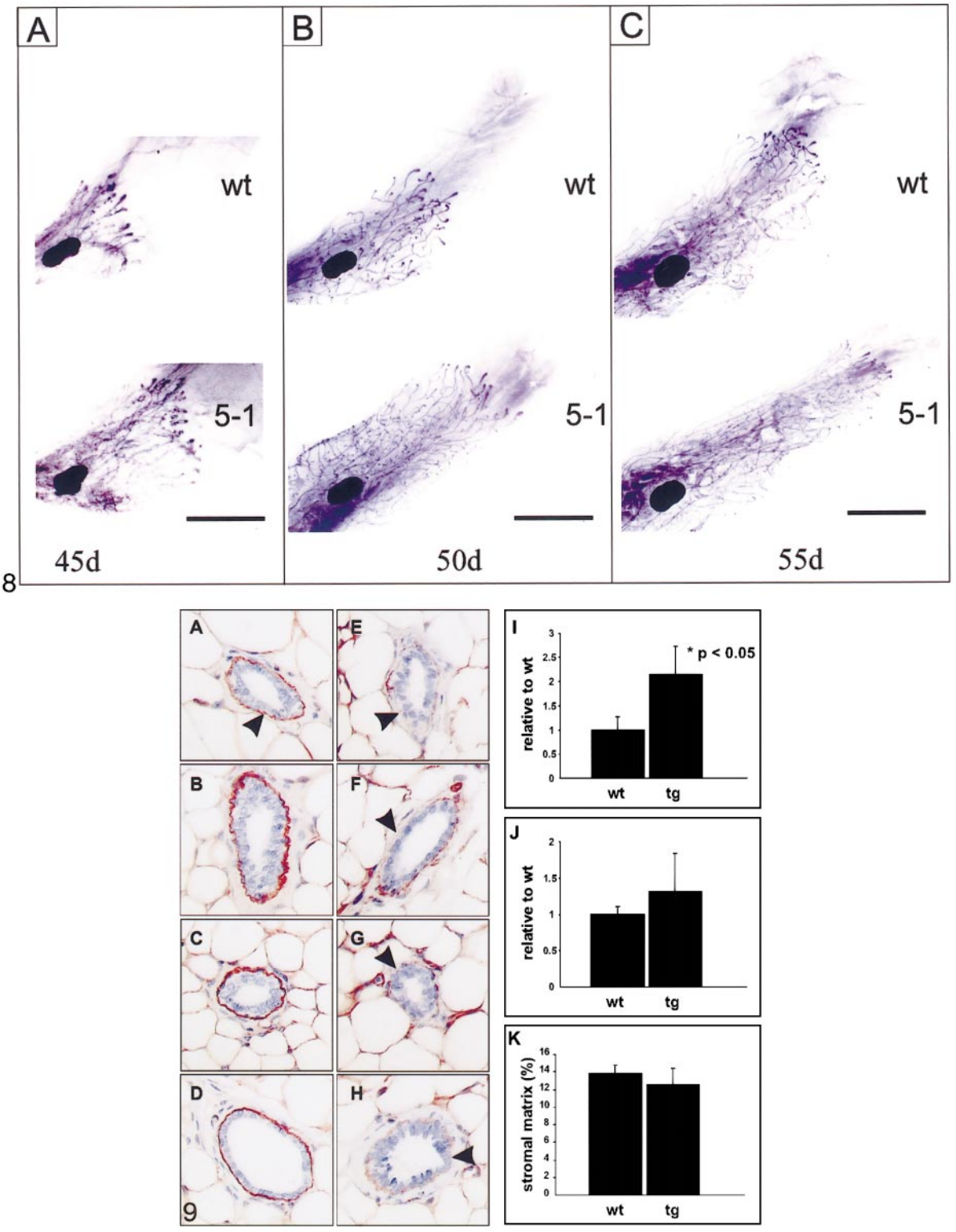

FIG. 8. Increased mammary ductal growth in *Timp-1*-reduced transgenic mammary tissue. (A–C) Whole-mounts of the fourth inguinal mammary fat pad from wild-type (wt) and transgenic (5-1) littermates at 45 (A), 50 (B), and 55 days (C). Scale bars, 0.5 cm.

and genetic methods to manipulate mammary *Timp-1* levels during this window of expression in order to elucidate the functional significance of its tightly regulated mammary expression. We demonstrated that a local rTIMP-1 elevation inhibited ductal elongation (Fig. 6) with no notable effect on basement membrane deposition in the approaching TEBs. In contrast, a reduction of mammary epithelial *Timp-1* in transgenic mice augmented linear ductal growth (Fig. 8) while not affecting the number of TEBs. This suggested that a down-regulation of *Timp-1* primarily affected lateral side branching and linear lengthening of epithelial ducts, but not TEB bifurcation. Further, we observed discontinuous laminin immunostaining in the basement membranes surrounding ducts (Fig. 9). We also showed that these biochemical and genetic manipulations led to altered epithelial proliferation (Fig. 10), with no effect on apoptosis. It is significant that a 50% reduction in epithelial *Timp-1* affected ductal morphogenesis, despite the abundance of other mammary *Timps.* This provides the first evidence that Timp-1 is able to affect epithelial proliferation *in vivo*. Further, the diminished epithelial basement membrane integrity during mammary morphogenesis likely contributes in part to increased proliferation, which in turn leads to increased linear lengthening and lateral side branching of ducts.

Since both forward expansion and lateral branching of mouse mammary ducts requires continuous remodeling of matrix molecules (Williams *et al.*, 1983; Silberstein and Daniel, 1982), matrix-specific proteases would facilitate these dynamic events by removing impeding basement membrane and connective tissue matrix. In support of this, we observed an abundance of active MMP-2 and MMP-9 (Fig. 5), indicating that basement membrane degradation is an ongoing process during the period of active ductal expansion and branching. Others have shown that endogenous MMP-3 mRNA localizes to stromal cells along the length of advancing ducts (Witty *et al.*, 1995) and that transgenic mammary expression of autoactivated MMP-3 leads to supernumerary branching from primary ducts (Sympson *et al.*, 1994; Witty *et al.*, 1995). We propose that the abundance of all four *Timps* is largely responsible for shielding this environment from excessive MMP-mediated matrix degradation, resulting in controlled remodeling. Our ability to manipulate ductal expansion by altering *Timp-1* levels strongly implicated Timp-1 as a regulator of MMP-facilitated mammary ductal expansion.

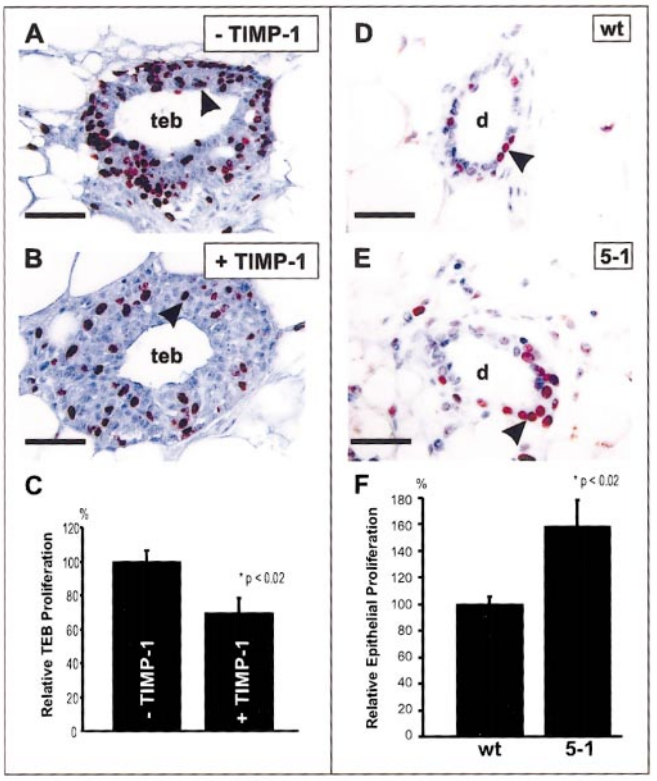

FIG. 10. Immunohistochemical analysis of proliferation in Timp-manipulated mouse mammary tissue. (A,B) BrdU immunostaining of TEBs (teb) in 40-day-old contralateral mammary tissue containing either an inert pellet (A, −TIMP-1) or an rTIMP-1-releasing pellet (B, +TIMP-1); arrowheads indicate positive-stained cell. (C) Percentage of BrdU-positive cells in TEBs from 40-day-old unmanipulated mice (represented as 100%, −TIMP-1) versus tissue containing rTIMP-1 pellets (+TIMP-1), determined by morphometric analysis. (D,E) PCNA immunostaining of mammary ductal (d) epithelial cells in 55-day wild type (D) and its transgenic littermate (E); positive-stained cells indicated by arrowheads. (F) Percentage of PCNA-positive cells in wild-type (represented as 100%) versus 5-1 transgenic mammary tissue, determined by morphometric analysis. Scale bars, 50 μm.

The degradation of basement membrane may influence the mammary microenvironment in several ways. First, it may remove impeding structural proteins, making way for

FIG. 9. Characterization of laminin, collagen type IV, and total stromal matrix in *Timp-1*-reduced mammary tissue and wild types. (A–D) Laminin immunostaining (arrowhead) on wild-type mammary tissue showing that epithelial ducts are completely encapsulated by a continuous, darkly stained basement membrane. (E–H) Laminin immunostaining on transgenic mammary tissue down-regulated in *Timp-1*. Epithelial ducts are often surrounded by discontinuous, diffuse, or lighter staining basement membrane (arrowheads). (I) Number of epithelial ducts in *Timp-1*-reduced mammary tissue (tg) surrounded by discontinuous laminin immunostaining relative to wild-type (wt) control littermates. (J) Number of epithelial ducts in *Timp-1*-reduced mammary tissue surrounded by discontinuous collagen type IV immunostaining relative to wild-type control littermates. (K) Percentage of mammary tissue constituted by total stromal matrix (Masson's trichrome staining) in wt and tg.

cellular migration and invasion. Second, it may release growth-promoting or -inhibiting factors sequestered within. Third, it may decrease the cell–ECM contacts needed for cell survival. Finally, it may reveal cryptic sites on degradation products, which in turn can influence cellular function. The main structural components of basement membrane are collagen type IV and the glycoprotein laminin. Several matrix metalloproteinases are capable of degrading laminin and collagen IV. These include the gelatinases (MMP-2 and -9; Okada *et al.,* 1990; Morodomi *et al.,* 1992), stromelysin-1 (MMP-3; Okada *et al.,* 1987), matrilysin (MMP-7; Wilson and Matrisian, 1996), metalloelastase (MMP-12; Chandler *et al.,* 1996) collagenase-3 (MMP-13; Knauper *et al.,* 1997), and MT-MMPs (MMP-14 to -17; d'Ortho *et al.,* 1997). The ability of Timps to inhibit these proteinases implicates them as strong candidates in conserving basement membrane integrity and function. We observed discontinuous, diffuse, or lighter laminin immunostaining, but not a decrease in total stromal matrix content in *Timp-1*-reduced transgenic tissue (Fig. 9). Aberrant laminin staining is likely a result of excessive MMP activity in the vicinity of basement membrane. *In vitro,* mammary epithelial cells are known to secrete MMPs vectorially toward basement membranes (Talhouk *et al.,* 1991). We suggest that epithelial-derived *Timp-1* reduction leads to a shift in the Timp/MMP balance, increasing MMP activity with local effects on the basement membrane microenvironment, while sparing stromal matrix turnover which may be more closely linked to the proteinase activity secreted by stromal fibroblasts. It is surprising that rTIMP-1 release did not influence matrix deposition around migrating TEBs, given that these structures normally have a minimal basement membrane at their tip (Silberstein *et al.,* 1982). It is possible that rTIMP-1 elevation during ductal development retarded TEB proliferation independent of matrix perturbation or that MMPs are not the primary proteinases responsible for basement membrane remodeling at the tip of TEBs. For example, the plasmin activator/plasmin system may be involved in matrix remodeling at the TEB forefront since urokinase plasminogen activator mRNA has been localized to the tips of epithelial cells migrating in three-dimensional collagen gels, with levels correlating to invasiveness (Delannoy-Courdent *et al.,* 1996).

Our investigations showed that an elevation of mammary Timp-1 inhibited mammary epithelial proliferation *in vivo,* but did not affect matrix deposition. We have also recently found in a liver tumor model that an elevation of hepatic Timp-1 inhibited transformation-associated hepatocyte hyperplasia *in vivo* with no overt affects on matrix deposition (Martin *et al.,* 1999). In light of the emerging concept that MMP activity can release growth factors bound to matrix molecules or cell membranes (Whitelock *et al.,* 1996; Gearing *et al.,* 1995) and process growth factor binding proteins (Thrailkill *et al.,* 1995; Fowlkes *et al.,* 1994a, b), it is conceivable that MMPs can increase, while Timps can inhibit, the amount of free growth factors within the cellular microenvironment. Reports of cellular hyperplasia following mammary MMP-3 (Witty *et al.,* 1995; Sympson *et al.,* 1994) or epidermal MMP-1 (D'armiento *et al.,* 1995) expression in other transgenic mice support this concept and are consistent with our findings in liver and mammary tissue up-regulated in Timp-1. In our liver tumor model, we have found that increased levels of hepatic Timp-1 suppressed hepatocellular carcinoma by inhibiting the MMP-mediated release of insulin-like growth factor-II (IGF-II) from the IGF-II:IGF-binding-protein-3 complex (D. C. Martin and R. Khokha, unpublished results). IGFs are important mitogens for mammary epithelial proliferation both during mammary development and during tumorigenesis (Ruan *et al.,* 1995). Changes in the levels of IGF or other growth factors accompanying mammary Timp manipulations during ductal development are currently being investigated.

The ECM is crucial to the maintenance of normal epithelial cell polarity and function in mammary cell cultures (Hay, 1993; Lin and Bissell, 1993). As well, changes in the ECM affect mammary epithelial gene expression (Lin *et al.,* 1995; Streuli *et al.,* 1995; Lee *et al.,* 1985), proliferation (Petersen *et al.,* 1992), and apoptosis (Boudreau *et al.,* 1996; Day *et al.,* 1997). For example, excessive ECM degradation and/or the loss of cell–ECM contacts induce apoptosis in mammary epithelial cells during mammary involution (Boudreau *et al.,* 1996; Talhouk *et al.,* 1992; Day *et al.,* 1997), an event shown to be rescued by Timp-1 (Talhouk *et al.,* 1992; Alexander *et al.,* 1996b). If this was also the case during virgin ductal development, we would anticipate that antisense down-regulation of *Timp-1* would induce MMP-mediated basement membrane degradation thereby inducing epithelial apoptosis and decreasing ductal expansion. However, our investigations showed that Timp-1 reduction did lead to loss of basement membrane integrity but did not promote mammary epithelial apoptosis. This may be due to three reasons. First, virgin mammary morphogenesis naturally has nonexistent apoptosis. Second, mammary epithelial apoptosis has largely been demonstrated in secretory alveolar epithelia isolated from gestational tissue that is distinct from virgin luminal epithelia. It is possible that the latter is more resistant to changes in cell–ECM contact. This is because secretory alveolar epithelia are surrounded by interspersed myoepithelia and have more contacts with basement membrane while luminal epithelial cells are almost completely encapsulated by myoepithelial cells and thus maintain fewer basement membrane contacts (Warburton *et al.,* 1982). Finally, our transgenic manipulation has not led to a complete loss of basement membrane, instead it has altered this structure only in localized areas.

In breast cancer, ductal carcinoma *in situ* is surrounded by an intact basement membrane and progression to malignant invasive ductal carcinoma is facilitated by MMP-mediated protease activity (Engel *et al.,* 1994; Davies *et al.,* 1993; Monteagudo *et al.,* 1990; Heppner *et al.,* 1996). The functional significance of *Timp* expression in breast cancer, however, is controversial. Due to the presence of high Timp-1 levels in breast cancer specimens (Yoshiji *et al.,*

1996) and the growth-promoting capabilities of Timp-1 *in vitro*, especially of the human breast cancer cell line MCF-7 (Hayakawa *et al.*, 1992), it has been suggested that Timp-1 promotes tumorigenicity. Contrary to this, transfection of *Timps* in tumorigenic cells has led to reduced malignancy, documenting a tumor-suppressive role for Timps (Khokha, 1994). Here we present the first report that examines directly the effects of Timp-1 on mammary ductal growth *in vivo*. We clearly demonstrate a significant inhibition of mammary epithelial proliferation upon *Timp-1* up-regulation with slow-release pellets (Figs. 10A–10C). Furthermore, we observed the opposite effect of increased epithelial proliferation with a *Timp-1* down-regulation in transgenic mammary tissue (Figs. 10D–10F). Although developmental and cancer events cannot be compared directly, there are parallels, and developmental studies have often been utilized to gain a basic understanding of cancer biology. Given our results, we propose that high Timp-1 levels seen in breast cancer may be a tissue response to increased MMP activity. Identification of factors that influence epithelial proliferation *in vivo* is of prime importance since breast cancer initiates in epithelial cells.

Human biology is thought to be affected by Timps at many levels, such as bone growth (Cawston, 1998), embryo implantation (Alexander *et al.*, 1996a), ovulation (McIntush and Smith, 1998), emphysema (Ohnishi *et al.*, 1998), arthritis (Airola *et al.*, 1998), tumorigenesis (Stetler-Stevenson *et al.*, 1996), angiogenesis (Sang, 1998), and metastasis (Liotta *et al.*, 1991). Timps are grouped as a family because of their conserved regions that allow them to bind with MMPs and inhibit their activity. However, major differences do exist between family members with respect to their MMP-binding constants (Hutton *et al.*, 1998; Taylor *et al.*, 1996), promoter elements (Borden and Heller, 1997), localization after secretion (Leco *et al.*, 1994), and tissue-specific expression (Leco *et al.*, 1997). Since all Timps are abundant in mammary tissue, unlike most other organs, it becomes increasingly important to understand the functional uniqueness of each Timp *in vivo* in breast tissue. Here, we have demonstrated that manipulation of a single Timp, Timp-1, functioned to affect the fundamental process of epithelial proliferation. It remains to be seen whether other Timps will affect this developmental event in a similar manner.

ACKNOWLEDGMENTS

The authors thank Drs. P. Waterhouse and M. L. Weir for critically reading the manuscript. This work was supported by grants from the Medical Research Council of Canada, the Canadian Breast Cancer Foundation, and the Human Frontier Science Program. J.E.F. is supported by a University of Toronto Open Scholarship and a Princess Margaret Hospital Graduate Scholarship, K.J.L. is a Helena Lam Scholar, R.A.M. is supported by a Knudson Cancer Research Fellowship, and D.C.M. was supported by an Ontario Graduate Scholarship.

REFERENCES

Airola, K., Ahonen, M., Johansson, N., Heikkila, P., Kere, J., Kahari, V. M., and Saarialho-Kere, U. K. (1998). Human TIMP-3 is expressed during fetal development, hair growth cycle, and cancer progression. *J. Histochem. Cytochem.* **46,** 437–447.

Alexander, C. M., Hansell, E. J., Behrendtsen, O., Flannery, M. L., Kishnani, N. S., Hawkes, S. P., and Werb, Z. (1996a). Expression and function of matrix metalloproteinases and their inhibitors at the maternal–embryonic boundary during mouse embryo implantation. *Development* **122,** 1723–1736.

Alexander, C. M., Howard, E. W., Bissell, M. J., and Werb, Z. (1996b). Rescue of mammary epithelial cell apoptosis and entactin degradation by a tissue inhibitor of metalloproteinases-1 transgene. *J. Cell Biol.* **135,** 1669–1677.

Bertaux, B., Hornebeck, W., Eisen, A. Z., and Dubertret, L. (1991). Growth stimulation of human keratinocytes by tissue inhibitor of metalloproteinases. *J. Invest. Dermatol.* **97,** 679–685.

Borden, P., and Heller, R. (1997). Transcriptional control of matrix metalloproteinases and the tissue inhibitors of matrix metalloproteinases. *Crit. Rev. Eukaryotic Gene Expression* **7,** 159–178.

Boudreau, N., Werb, Z., and Bissell, M. J. (1996). Suppression of apoptosis by basement membrane requires three-dimensional tissue organization and withdrawal from the cell cycle. *Proc. Natl. Acad. Sci. USA* **93,** 3509–3513.

Cawston, T. (1998). Matrix metalloproteinases and TIMPs: Properties and implications for the rheumatic diseases. *Mol. Med. Today* **4,** 130–137.

Chandler, S., Cossin, J., Lury, J., and Wells, G. (1996). Macrophage metalloelastase degrades matrix and myelin proteins and processes a tumour necrosis factor-α fusion protein. *Biochem. Biophys. Res. Commun.* **228,** 421–429.

Chomczynski, P., and Sacchi, N. (1987). Single-step method of RNA isolation by acid guanidinium thiocyanate–phenol–chloroform extraction. *Anal. Biochem.* **162,** 156–159.

Church, G. M., and Gilbert, W. (1984). Genomic sequencing. *Proc. Natl. Acad. Sci. USA* **81,** 1991–1995.

D'armiento, J., DiColandrea, T., Dalal, S. S., Okada, Y., Huang, M. T., Conney, A. H., and Chada, K. (1995). Collagenase expression in transgenic mouse skin causes hyperkeratosis and acanthosis and increases susceptibility to tumorigenesis. *Mol. Biol. Cell* **10,** 5732–5739.

d'Ortho, M. P., Will, H., Atkinson, S., Butler, G., Messent, A., Gravilovic, J., Smith, B., Timpl, R., Zardi, L., and Murphy, G. (1997). Membrane-type matrix metalloproteinases 1 and 2 exhibit broad-spectrum proteolytic capacities comparable to many matrix metalloproteinases. *Eur. J. Biochem.* **250,** 751–757.

Daniel, C. W., and Silberstein, G. B. (1987). Postnatal development of the rodent mammary gland. *In* "The Mammary Gland: Development, Regulation, and Function" (M. C. Neville and C. W. Daniel, Eds.), pp. 3–31. Plenum, New York.

Davies, B., Miles, D. W., Happerfield, L. C., Naylor, M. S., Bobrow, L. G., Rubens, R. D., and Balkwill, F. R. (1993). Activity of type IV collagenases in benign and malignant breast disease. *Br. J. Cancer* **67,** 1126–1131.

Day, M. L., Foster, R. G., Day, K. C., Zhao, X., Humphrey, P., Swanson, P., Postigo, A. A., Zhang, S. H., and Dean, D. C. (1997). Cell anchorage regulates apoptosis through the retinoblastoma tumor suppressor/E2F pathway. *J. Biol. Chem.* **272,** 8125–8128.

Delannoy-Courdent, A., Fauquette, W., Dong-Le, B. X., Boilly, B., Vandenbunder, B., and Desbiens, X. (1996). Expression of c-ets-1 and uPA genes is associated with mammary epithelial cell

tubulogenesis or neoplastic scattering. *Int. J. Dev. Biol.* **40,** 1097–1108.

Delannoy-Courdent, A., Mattot, V., Fafeur, V., Fauquette, W., Pollet, I., Calmels, T., Vercamer, C., Boilly, B., Vandenbunder, B., and Desbiens, X. (1998). The expression of an Ets1 transcription factor lacking its activation domain decreases uPA proteolytic activity and cell motility, and impairs normal tubulogenesis and cancerous scattering in mammary epithelial cells. *J. Cell Sci.* **111,** 1521–1534.

Dulbecco, R., Allen, W. R., Bologna, M., and Bowman, M. (1986). Marker evolution during the development of the rat mammary gland: Stem cells identified by markers and the role of myoepithelial cells. *Cancer Res.* **46,** 2449–2456.

Edwards, D. R., Waterhouse, P., Holman, M. L., and Denhardt, D. T. (1986). A growth-responsive gene (16C8) in normal mouse fibroblasts homologous to a human collagenase inhibitor with erythroid-potentiating activity: Evidence for inducible and constitutive transcripts. *Nucleic Acids Res.* **14,** 8863–8878.

Engel, G., Heselmeyer, K., Auer, G., Backdahl, M., Eriksson, E., and Linder, S. (1994). Correlation between stromelysin-3 mRNA level and outcome of human breast cancer. *Int. J. Cancer* **58,** 830–835.

Fauquette, W., Dong-Le, B. X., Delannoy-Courdent, A., Boilly, B., and Desbiens, X. (1997). Characterization of morphogenetic and invasive abilities of human mammary epithelial cells: Correlation with variations of urokinase-type plasminogen activator activity and type-1 plasminogen activator inhibitor level. *Biol. Cell* **89,** 453–465.

Fowlkes, J. L., Enghild, J. J., Suzuki, K., and Nagase, H. (1994a). Matrix metalloproteinases degrade insulin-like growth factor-binding protein-3 in dermal fibroblast cultures. *J. Biol. Chem.* **269,** 25742–25746.

Fowlkes, J. L., Suzuki, K., Nagase, H., and Thrailkill, K. M. (1994b). Proteolysis of insulin-like growth factor binding protein-3 during rat pregnancy: A role for matrix metalloproteinases. *Endocrinology* **135,** 2810–2813.

Gearing, A. J., Beckett, P., Christodoulou, M., Churchill, M., Clements, J. M., Crimmin, M., Davidson, A. H., Drummond, A. H., Galloway, W. A., Gilbert, R., *et al.* (1995). Matrix metalloproteinases and processing of pro-TNF-alpha. *J. Leukocyte Biol.* **57,** 774–777.

Gomez, D. E., Alonso, D. F., Yoshiji, H., and Thorgeirsson, U. P. (1997). Tissue inhibitors of metalloproteinases: Structure, regulation and biological functions. *Eur. J. Cell Biol.* **74,** 111–122.

Harvey, M. B., Leco, K. J., Arcellana-Panlilio, M. Y., Zhang, X., Edwards, D. R., and Schultz, G. A. (1995). Proteinase expression in early mouse embryos is regulated by leukaemia inhibitory factor and epidermal growth factor. *Development* **121,** 1005–1014.

Haslam. (1987). Role of sex steroid hormones in normal mammary gland function. *In* "The Mammary Gland: Development, Regulation, and Function" (E. Niskanen and C. W. Daniel, Eds.), pp. 499–510. Plenum, New York.

Hay, E. D. (1993). Extracellular matrix alters epithelial differentiation. *Curr. Opin. Cell Biol.* **5,** 1029–1035.

Hayakawa, T., Yamashita, K., Ohuchi, E., and Shinagawa, A. (1994). Cell growth-promoting activity of tissue inhibitor of metalloproteinases-2 (TIMP-2). *J. Cell Sci.* **107,** 2373–2379.

Hayakawa, T., Yamashita, K., Tanzawa, K., Uchijima, E., and Iwata, K. (1992). Growth-promoting activity of tissue inhibitor of metalloproteinases-1 (TIMP-1) for a wide range of cells. A possible new growth factor in serum. *FEBS Lett.* **298,** 29–32.

He, C., Wilhelm, M. W., Pentland, A. P., Marmer, B. I., Grant, G. A., Eisen, A. Z., and Goldberg, G. I. (1986). Tissue cooperation in a proteolytic cascade activating human interstitial collagenase. *Proc. Natl. Acad. Sci. USA* **86,** 2632–2636.

Heppner, K. J., Matrisian, L. M., Jensen, R. A., and Rodgers, W. H. (1996). Expression of most matrix metalloproteinase family members in breast cancer represents a tumor-induced host response. *Am. J. Pathol.* **149,** 273–282.

Hogan, B., Costantini, F., and Lacy, E. (1986). Introduction of new genetic information into the developing mouse embryo. *In* "Manipulating the Mouse Embryo" (B. Hogan, F. Costantini, and E. Lacy, Eds.), pp. 153–197. Cold Spring Harbor Laboratory Press, New York.

Hutton, M., Willenbrock, F., Brocklehurst, K., and Murphy, G. (1998). Kinetic analysis of the mechanism of interaction of full-length TIMP-2 and gelatinase A: Evidence for the existence of a low-affinity intermediate. *Biochemistry* **37,** 10094–10098.

Imagawa, W., Bandyopadhyay, G. K., and Nandi, S. (1990). Regulation of mammary epithelial cell growth in mice and rats. *Endocr. Rev.* **11,** 494–523.

Inderdeo, D. S., Edwards, D. R., Han, V. K., and Khokha, R. (1996). Temporal and spatial expression of tissue inhibitors of metalloproteinases during the natural ovulatory cycle of the mouse. *Biol. Reprod.* **55,** 498–508.

Jones, F. E., Jerry, D. J., Guarino, B. C., Andrews, G. C., and Stern, D. F. (1996). Heregulin induces in vivo proliferation and differentiation of mammary epithelium into secretory lobuloalveoli. *Cell Growth Differ.* **7,** 1031–1038.

Khokha, R. (1994). Suppression of the tumorigenic and metastatic abilities of murine B16-F10 melanoma cells in vivo by the overexpression of the tissue inhibitor of metalloproteinases-1. *J. Natl. Cancer Inst.* **86,** 299–304.

Knauper, V., Cowell, S., Smith, B., Lopez-Otin, C., O'Shea, M., Morris, H., Zardi, L., and Murphy, G. (1997). The role of the C-terminal domain of human collagenase-3 (MMP-13) in the activation of procollagenase-3, substrate specificity, and tissue inhibitor of metalloproteinase interaction. *J. Biol. Chem.* **272,** 7608–7616.

Kruger, A., Fata, J. E., and Khokha, R. (1997). Altered tumor growth and metastasis of a T-cell lymphoma in Timp-1 transgenic mice. *Blood* **90,** 1993–2000.

Langer, R., and Folkman, J. (1976). Polymers for the sustained release of proteins and other macromolecules. *Nature* **263,** 797–800.

Leco, K. J., Apte, S. S., Taniguchi, G. T., Hawkes, S. P., Khokha, R., Schultz, G. A., and Edwards, D. R. (1997). Murine tissue inhibitor of metalloproteinases-4 (Timp-4): cDNA isolation and expression in adult mouse tissues. *FEBS Lett.* **401,** 213–217.

Leco, K. J., Khokha, R., Pavloff, N., Hawkes, S. P., and Edwards, D. R. (1994). Tissue inhibitor of metalloproteinases-3 (TIMP-3) is an extracellular matrix-associated protein with a distinctive pattern of expression in mouse cells and tissues. *J. Biol. Chem.* **269,** 9352–9360.

Lee, E. Y., Lee, W. H., Kaetzel, C. S., Parry, G., and Bissell, M. J. (1985). Interaction of mouse mammary epithelial cells with collagen substrata: Regulation of casein gene expression and secretion. *Proc. Natl. Acad. Sci. USA* **82,** 1419–1423.

Lin, C. Q., and Bissell, M. J. (1993). Multi-faceted regulation of cell differentiation by extracellular matrix. *FASEB J.* **7,** 737–743.

Lin, C. Q., Dempsey, P. J., Coffey, R. J., and Bissell, M. J. (1995). Extracellular matrix regulates whey acidic protein gene expression by suppression of TGF-alpha in mouse mammary epithelial cells: Studies in culture and in transgenic mice. *J. Cell Biol.* **129,** 1115–1126.

Liotta, L. A., Steeg, P. S., and Stetler-Stevenson, W. G. (1991). Cancer metastasis and angiogenesis: An imbalance of positive and negative regulation. *Cell.* **64,** 327–336.

Martin, D. C., Sanchez-Sweatman, O. H., Ho, A., Inderdeo, D. S., Tsao, M., and Khokha, R. (1999). Transgenic TIMP-1 inhibits simian virus 40 T antigen-induced hepatocarcinogenesis by impairment of hepatocellular proliferation and tumor angiogenesis. *Lab. Invest.* **79,** 1–10.

Martinez-Hernandez, A., Louis, M. D., Fink, M. D., and Pierce, G. B. (1976). Removal of basement membrane in the involuting breast. *Lab. Invest.* **34,** 455–462.

McIntush, E. W., and Smith, M. F. (1998). Matrix metalloproteinases and tissue inhibitors of metalloproteinases in ovarian function. *Rev. Reprod.* **3,** 23–30.

Melton, D., Kreig, P., Rebagliati, M. R., Maniatis, T., Zinn, K., and Green, M. R. (1984). Efficient in vitro synthesis of biologically active RNA and RNA hybridization probes from plasmids containing a bacteriophage SP6 promoter. *Nucleic Acids Res.* **12,** 7035–7056.

Mignatti, P., and Rifkin, D. B. (1993). Biology and biochemistry of proteinases in tumor invasion. *Physiol. Rev.* **73,** 161–195.

Monteagudo, C., Merino, M. J., San-Juan, J., Liotta, L. A., and Stetler-Stevenson, W. G. (1990). Immunohistochemical distribution of type IV collagenase in normal, benign, and malignant breast tissue. *Am. J. Pathol.* **136,** 585–592.

Montgomery, A. M., Mueller, B. M., Reisfeld, R. A., Taylor, S. M., and DeClerck, Y. A. (1994). Effect of tissue inhibitor of the matrix metalloproteinases-2 expression on the growth and spontaneous metastasis of a human melanoma cell line. *Cancer Res.* **54,** 5467–5473.

Morodomi, T., Ogata, Y., Sasaguri, Y., Morimatsu, M., and Nagase, H. (1992). Purification and characterization of matrix metalloproteinase 9 from U937 monocytic leukaemia and HT1080 fibrosarcoma cells. *Biochem. J.* **285,** 603–611.

Muller, W. J., Sinn, E., Pattengale, P. K., Wallace, R., and Leder, P. (1988). Single-step induction of mammary adenocarcinoma in transgenic mice bearing the activated c-neu oncogene. *Cell* **54,** 105–115.

Ohnishi, K., Takagi, M., Kurokawa, Y., Satomi, S., and Konttinen, Y. (1998). Matrix metalloproteinase-mediated extracellular matrix protein degradation in human pulmonary emphysema. *Lab. Invest.* **78,** 1077–1087.

Okada, Y., Morodomi, T., Enghild, J. J., Suzuki, K., Yasui, A., Nakanishi, I., Salvesen, G., and Nagase, H. (1990). Matrix metalloproteinase 2 from human rheumatoid synovial fibroblasts. Purification and activation of the precursor and enzymic properties. *Eur. J. Biochem.* **194,** 721–730.

Okada, Y., Nagase, H., and Harris, E. (1987). Matrix metalloproteinases 1, 2, and 3 from rheumatoid synovial cells are sufficient to destroy joints. *J. Rheumatol.* **14,** 41–42.

Pattengale, P. K., Stewart, T. A., Leder, A., Sinn, E., Muller, W., Tepler, I., Schmidt, E., and Leder, P. (1989). Animal models of human disease. Pathology and molecular biology of spontaneous neoplasms occurring in transgenic mice carrying and expressing activated cellular oncogenes. *Am. J. Pathol.* **135,** 39–61.

Petersen, O. W., Ronnov-Jessen, L., Howlett, A. R., and Bissell, M. J. (1992). Interaction with basement membrane serves to rapidly distinguish growth and differentiation pattern of normal and malignant human breast epithelial cells [published erratum appears in *Proc. Natl. Acad. Sci. USA*, 1993, **90,** 2556]. *Proc. Natl. Acad. Sci. USA* **89,** 9064–9068.

Rhine, W. D., Hsieh, D. S. T., and Langer, R. (1980). Polymers from sustained macromolecule release: Procedures to fabricate reproducible delivery systems and control release kinetics. *J. Pharm. Sci.* **69,** 265–270.

Ruan, W., Catanese, V., Wieczorek, R., Feldman, M., and Kleinberg, D. L. (1995). Estradiol enhances the stimulatory effect of insulin-like growth factor-I (IGF-I) on mammary development and growth hormone-induced IGF-I messenger ribonucleic acid. *Endocrinology* **136,** 1296–1302.

Sang, Q. (1998). Complex role of matrix metalloproteinases in angiogenesis. *Cell Res.* **8,** 171–177.

Silberstein, G. B., and Daniel, C. W. (1982). Glycosaminoglycans in the basal lamina and extracellular matrix of the developing mouse mammary duct. *Dev. Biol.* **90,** 215–222.

Sonnenberg, A., Daams, H., Van der Valk, M. A., Hilkens, J., and Hilgers, J. (1986). Development of mouse mammary gland: Identification of stages in differentiation of luminal and myoepithelial cells using monoclonal antibodies and polyvalent antiserum against keratin. *J. Histochem. Cytochem.* **34,** 1037–1046.

Stetler-Stevenson, W. G., Bersch, N., and Golde, D. W. (1992). Tissue inhibitor of metalloproteinase-2 (TIMP-2) has erythroid-potentiating activity. *FEBS Lett.* **296,** 231–234.

Stetler-Stevenson, W. G., Hewitt, R., and Corcoran, M. L. (1996). Matrix metalloproteinases and tumor invasion: From correlation and causality to the clinic. *Semin. Cancer Biol.* **7,** 147–154.

Stetler-Stevenson, W. G., Krutzsch, H. C., and Liotta, L. A. (1989). Tissue inhibitor of metalloproteinase (TIMP-2). A new member of the metalloproteinase inhibitor family. *J. Biol. Chem.* **264,** 17374–17378.

Streuli, C. H., Schmidhauser, C., Bailey, N., Yurchenco, P., Skubitz, A. P., Roskelley, C., and Bissell, M. J. (1995). Laminin mediates tissue-specific gene expression in mammary epithelia. *J. Cell Biol.* **129,** 591–603.

Sympson, C. J., Talhouk, R. S., Alexander, C. M., Chin, J. R., Clift, S. M., Bissell, M. J., and Werb, Z. (1994). Targeted expression of stromelysin-1 in mammary gland provides evidence for a role of proteinases in branching morphogenesis and the requirement for an intact basement membrane for tissue-specific gene expression. *J. Cell Biol.* **125,** 681–693.

Talhouk, R. S., Bissell, M. J., and Werb, Z. (1992). Coordinated expression of extracellular matrix-degrading proteinases and their inhibitors regulates mammary epithelial function during involution. *J. Cell Biol.* **118,** 1271–1282.

Talhouk, R. S., Chin, J. R., Unemori, E. N., Werb, Z., and Bissell, M. J. (1991). Proteinases of the mammary gland: Developmental regulation in vivo and vectorial secretion in culture. *Development* **112,** 439–449.

Taylor, K. B., Windsor, L. J., Caterina, N. C. M., Bodden, M. K., and Engler, J. A. (1996). The mechanism of inhibition of collagenase by TIMP-1. *J. Biol. Chem.* **271,** 23938–23945.

Thrailkill, K. M., Quarles, L. D., Nagase, H., Suzuki, K., Serra, D. M., and Fowlkes, J. L. (1995). Characterization of insulin-like growth factor-binding protein 5-degrading proteases produced throughout murine osteoblast differentiation. *Endocrinology* **136,** 3527–3533.

Vassilacopoulou, D., and Boylan, E. S. (1993). Mammary gland morphology and responsiveness to regulatory molecules following prenatal exposure to diethylstilbestrol. *Teratog. Carcinog. Mutagen.* **13,** 59–74.

Warburton, M. H., Mitchell, D., Ormerod, E. J., and Rudland, P. (1982). Distribution of myoepithelial cells and basement membrane proteins in the resting, pregnant, lactating, and involuting rat mammary gland. *J. Histochem. Cytochem.* **30,** 667–676.

Whitelock, J. M., Murdoch, A. D., Iozzo, R. V., and Underwood, P. A. (1996). The degradation of human endothelial cell-derived perlecan and release of bound basic fibroblast growth factor by stromelysin, collagenase, plasmin, and heparanases. *J. Biol. Chem.* **271,** 10079–10086.

Wijsman, J. H., Jonker, R. R., Keijzer, R., Van De Velde, C. J. H., Cornelisse, C. J., and Van Dierendonck, J. H. (1993). A new method to detect apoptosis in paraffin sections: In situ end-labeling of fragmented DNA. *J. Histochem. Cytochem.* **1,** 7–12.

Williams, J. M., and Daniel, C. W. (1983). Mammary ductal elongation: Differentiation of myoepithelium and basal lamina during branching morphogenesis. *Dev. Biol.* **97,** 274–290.

Wilson, C. L., and Matrisian, L. M. (1996). Matrilysin: An epithelial matrix metalloproteinase with potentially novel functions. *Int. J. Biochem. Cell Biol.* **28,** 123–136.

Witty, J. P., Wright, J. H., and Matrisian, L. M. (1995). Matrix metalloproteinases are expressed during ductal and alveolar mammary morphogenesis, and misregulation of stromelysin-1 in transgenic mice induces unscheduled alveolar development. *Mol. Biol. Cell.* **6,** 1287–1303.

Woessner, J. F. (1991). Matrix metalloproteinases and their inhibitors in connective tissue remodeling. *FASEB J.* **5,** 2145–2154.

Yoshiji, H., Gomez, D. E., and Thorgeirsson, U. P. (1996). Enhanced RNA expression of tissue inhibitor of metalloproteinases-1 (TIMP-1) in human breast cancer. *Int. J. Cancer.* **69,** 131–134.

Received for publication November 18, 1998
Revised April 23, 1999
Accepted April 23, 1999